

Document downloaded from:

<http://hdl.handle.net/10251/63797>

This paper must be cited as:

Kamaraj, S.; Mollá Romano, S.; Compañ Moreno, V.; Poggi-Varaldo, HM.; Solorza-Feria, O. (2015). Use of Novel Reinforced Cation Exchange Membranes for Microbial Fuel Cells. *Electrochimica Acta*. 176:555-566. doi:10.1016/j.electacta.2015.07.042.



The final publication is available at

<http://dx.doi.org/10.1016/j.electacta.2015.07.042>

Copyright Elsevier

Additional Information

Use of Novel Reinforced Cation Exchange Membranes for Microbial Fuel Cells

Sathish-Kumar Kamaraj^{1,2}, Sergio Mollá Romano³, Vicente Compañ Moreno^{3,*}, H.M. Poggi-Varaldo⁴, O. Solorza-Feria⁵

¹ Programa de nanociencias y Nanotecnología. Centro de Investigación y de Estudios Avanzados, CINVESTAV-IPN. Av. Instituto Politécnico Nacional 2508, Col. Zacatenco. 07360 D.F. México

² Present address- Programa de Ing. En Energía. Universidad Politécnica de Aguascalientes, Ags, 20342, Mexico

³Dpto. Termodinámica Aplicada, Universidad Politécnica de Valencia, 46022-Valencia, Spain

⁴Dpto. Biotecnología y Bioingeniería, CINVESTAV-IPN, 07360-México D.F., Mexico.

⁵Dpto. Química, CINVESTAV-IPN, 07360-México D.F., Mexico

Abstract

This work has been focused on the synthesis and characterization of different blended membranes SPEEK-35PVA (Water), SPEEK-35PVA (DMAc) prepared by casting and nanofiber-reinforced proton exchange membranes Nafion-PVA-15, Nafion-PVA-23 and SPEEK/PVA-PVB. The two first reinforced membranes were made up of Nafion® polymer deposited between polyvinyl alcohol (PVA) nanofibers. The last composite membrane is considered because the PVA is a hydrophilic polymer which forms homogeneous blends with SPEEK suitable to obtain high proton conductivity, while the hydrophobic PVB can produce blends in a phase separation morphology in which very low water uptake can be found. The synthesized membranes showed an outstanding stability, high proton conductivity, and enhanced mechanical and barrier properties. The membranes were characterized in single chamber microbial fuel cells (SCMFCs) using electrochemically enriched high sodic saline hybrid H-inocula (*Geobacter metallireducen*, *Desulfurivibrio alkaliphilus*, and *Marinobacter adhaerens*) as biocatalyst. The best performance was obtained with Nafion-PVA-15 membrane, which achieved a maximum power density of 1053 mW/m³ at a cell voltage of 340 mV and displayed the lowest total internal resistance ($R_{int} \approx 522 \Omega$). This result is in agreement with the low oxygen permeability and the moderate conductivity found in this kind of membranes. These results are encouraging towards obtaining high concentrated sodic saline model wastewater exploiting MFCs.

Keywords: Microbial fuel cells, SPEEK (sulfonated poly-ether-ether-ketone), Nafion reinforced membrane, High saline wastewater.

*: Corresponding author: Dr. Vicente Compañ. Tel.: +34963879328; Fax: +34963877924;
E-mail address: vicommo@ter.upv.es

1. Introduction

Microbial fuel cells (MFCs) have emerged as a promising technology for wastewater treatment as well as means of energy recovery by microorganisms, and they have become an intensive subject of research in bio-electrochemistry [1-6]. Electrochemically active bacteria in the anode chamber are oxidizing the diverse organic substrate, liberate electrons and protons. The electrons travel to the cathode site via an external circuit and protons diffuse through the proton exchange membrane (PEM). The protons and electrons subsequently combine at the cathode side with molecular oxygen, to produce water [7, 8]. The MFCs offer the possibility of extracting current mainly on each electron that are produced in the anode from a wide range of dissolved complex organic wastes and an equivalent amount of protons which must be transported to the cathode through the electrolyte to sustain the current. Therefore, PEMs are one of the most important components in MFCs as they physically separate the anode and cathode chambers, thereby avoiding undesirable crossover, while allowing protons to pass through to the cathode's side. In MFCs, the Nafion[®]117 membrane is one of the most commonly used PEM, though a number of problems associated with Nafion[®]117 arise, such as oxygen leakage from cathode to anode, substrate loss, cation (rather than protons) transport, and biofouling. Among these issues, one of the main problems is the oxygen leakage into the anode chamber, which can either inhibit the growth of obligate anaerobes or facilitate aerobic respiration by facultative bacteria, thus resulting in lower energy recovery, due to the substrate losses [9-13].

Nafion[®] membranes contains negatively charged sulfonated groups in the backbone of the polymer chains, which explains the high level of proton conductivity, while also showing a significant, undesirable affinity for other cations, rather than protons [14]. In general, MFCs are operated with a pH increasing as consequence of the amount of cations (Na^+ , K^+ , Ca^{2+} , Mg^{2+} and NH_4^+) contained in the growth medium, where they are typically present in concentrations about 100 times as high as that of protons. Subsequently, these cations combine with the sulfonated groups of Nafion[®] and inhibit the migration of protons produced during substrate degradation, causing a decrease in MFCs performance as a consequence of larger ohmic losses in the membrane, accompanied by a simultaneous pH reduction in the anode chamber and a corresponding pH increase in the cathode side

affecting electrode reactions [15]. The alkalinity at the cathode is due to the formation of OH⁻ from the ORR the layers have been applied outside. The performance of separator-less MFCs was also improved by modifying the configuration of their electrodes [16-18]. While novel nanofiber- reinforced membranes have reduced the cost of materials used in direct methanol fuel cells (DMFC) [19-21]. To our knowledge, there is no work up until now reported on the use of separators made of nanofiber-reinforced sulfonated membranes. In our study two different kinds of membranes have been investigated. On the one hand, composite membranes based on poly(ether ether ketone sulfonated) (SPEEK) and, on the other hand, Nafion® reinforced with poly(vinyl alcohol) PVA nanofibers that can produce significant savings in the consumed amount of Nafion® obtaining membranes of lower costs than other PEMs.

In this way, some authors of this manuscript have recently reported that the incorporation of polyvinyl alcohol (PVA) into a Nafion® matrix, obtained by electrospinning of a water solution of PVA with a cationic surfactant additive, is a suitable approach to obtain novel nanocomposite membranes with reduced methanol crossover [19-21]. The advantages exhibited by the nanofibers come from obtaining reinforced composite films much thinner than commercial Nafion® 117, which can be an attractive potential as oxygen barriers for membranes used in MFCs.

Additionally, sulfonated poly(ether-ether-ketone) (SPEEK) materials are potential candidates to replace Nafion® at low cost while exhibiting good thermal and chemical stability [22-24]. In this sense, studies carried out recently on blended SPEEK membranes with the addition of hydrophilic or hydrophobic polymers into SPEEK matrix has provided stability towards swelling. The incorporation of PVA (hydrophilic polymer) promoted the achievement of acceptable proton conductivities, while the addition of PVB (hydrophobic polymer) into the SPEEK matrix produced a barrier effect on the methanol [24], and therefore, a good performance is also foresees to reduce oxygen permeability.

The objective of a previous study of other members of this work was the comparison of three enrichment methods for soil inoculums from Texococo lake, México [6]. They characterized the purified inoculums with a single Nafion® 117 membrane . It was concluded that using electrochemically enriched high sodic saline hybrid H-inocula as biocatalyst achieved the best performance. However, the focus of this study is the

characterization of the optimized inoculums using four additional novel membranes. Two of them were prepared using the electrospinning technique, Nafion-PVA and SPEEK-30PVB-35PVA, and two of them are based on blends of SPEEK and PVA, obtained from different solvents, water (SPEEK-35PVA(Water)), and dimethylacetamide, (SPEEK-35PVA(DMAc)).

2. Experimental Section

2.1. Materials

Commercial Nafion[®] (20 wt% - DuPont Co) dispersion was solvent exchanged in order to prepare 5 wt% dispersion in an isopropanol/water mixture, 4:1 w/w, respectively. Granulated SPEEK (FUMION ionomers) with ionic exchange capacity (IEC) of 1.75 and 2.05 mmol/g was acquired from Fumatech GmbH (St. Ingbert, Germany). Polyvinyl alcohol (PVA), Mowiol 28-99 grade, and polyvinyl butyral, (PVB), were donated by Kuraray Europe GmbH (Frankfurt, Germany). Isopropanol, cetyltrimethylammonium bromide (CTAB) and dimethylacetamide (DMAc) were purchased from Acros Organics, while anhydrous lithium chloride and 4-formyl-1,3-benzenedisulfonic acid disodium salt was obtained from Sigma-Aldrich.

2.2. Preparation of Nafion-PVA membranes

2.2.1. PVA nanofibers and their chemical functionalization

The procedure has been described elsewhere [19-21]. Porous PVA mats were produced by a standard electrospinning setup (Yflow S.L., Málaga, Spain) through the feeding of a water based solution of PVA (0.04:1:10 wt. CTAB:PVA:water). The collected mats were heated during 3 hours at 170°C in a vacuum (250 mbar pressure) with the purpose of removing water and increasing manipulability. The PVA mats were fixed between round steel frames and immersed into a bath with a 0.04 M concentration of 4-formyl-1,3-benzenedisulfonic acid disodium salt and 0.1 M of chlorhydric acid as a catalyst [19-21].

2.2.2. Composite Nafion[®] membranes reinforced with PVA nanofibers

The nanofibers mats were impregnated with the 5 wt% Nafion[®] solution in isopropanol and water (4/1 w/w, respectively). Annealing was carried out at 125°C for 90 min under pressure (60 N cm⁻²) using a hot plate press (Rondol Hand Press 10, United Kingdom). More details of the experimental method are given in previous papers [19-21].

The thickness of the composite membranes (L) was dependent on the deposition time of the electrospun nanofiber mats, and it was measured with a digital length gauge (Heidenhain MT 12, Germany). The membranes thickness was calculated as the average value after ten measurements on different parts of the sample. The pertinent results are given in Table 1.

2.3. SPEEK-based membranes

2.3.1. Water-based SPEEK-35PVA membranes

SPEEK (ion-exchange capacity (IEC) of 1.75 meq/g) was dissolved in boiling water. An appropriate amount of PVA was separately dissolved in water at 80°C (10 wt% PVA concentration) and then both solutions were mixed to prepare a SPEEK-35PVA composite (35 wt% content) and water was added until reaching a 7.5 wt% total polymer concentration. The solution was stirred at room temperature until complete homogenization and the membranes cast on a Teflon[®] Petri dish left overnight in an oven at 40°C. Finally, the membranes were crosslinked at 120°C for 1 hour and placed in boiling water for another hour. The membranes were stored in water at room temperature.

2.3.2. DMAc-based SPEEK-35PVA membranes

Membranes were prepared by casting of solutions with a 10 wt% concentration of polymer blend (SPEEK+PVA) in DMAc solvent incorporating LiCl. Previously, LiCl was dissolved in DMAc at a 0.4 wt% concentration at room temperature. Then, the required amount of PVA was dissolved stirring at 140°C for 1 hour; afterwards, the solution was allowed to cool down to room temperature. Finally, SPEEK (IEC=1.75 meq/g) was added, and the solution stirred at 140°C for 1 hour in order to ensure a complete homogenization. Membranes were obtained by casting at 80°C on a Teflon[®] dish overnight, followed by a treatment at 140°C for 2 hours and an additional 1 hour at the same temperature under

vacuum with the purpose of enhancing the removal of trapped DMAc molecules. The last step was crosslinking between the SPEEK and the PVA chains at 200°C for 1 hour (without vacuum). It was observed that crosslinking did not take place below 170°C, in opposition to the behaviour of the water-based SPEEK-35PVA membranes. Finally, the crosslinked membranes were immersed in boiling water for 1 hour and stored in water at room temperature.

2.3.3. Synthesis of SPEEK-PVA-PVB composite membrane

2.3.3.1. SPEEK-30PVB nanofibers

First, a SPEEK solution containing 30 wt% PVB (SPEEK-30PVB) in DMAc was prepared as follows: A required amount of PVB was dissolved under stirring in DMAc at 80°C for 1 hour. The solution was let to cool down at room temperature, then SPEEK (IEC = 2.05 meq/g) was incorporated and the mixture stirred for 1 hour at 80°C until complete homogenization (17.5 wt% total polymer concentration).

Nanofiber mats of SPEEK-30PVB were obtained by electrospinning (YFLOW SL, Malaga, Spain). A potential difference of 35 kV was applied between the needle and the planar collector, which were separated 25 cm, and a flow rate of 0.2 ml h⁻¹ was fixed during the electrospinning process. After a 15 hour deposition, the mat was heated at 160°C for 30 minutes to remove trapped DMAc and then cross linked at 200 °C for 1 hour. Round steel frames (similar to the PVA nanofiber case) were placed on the surface of the PVB nanofibers with the aim of compensating the dimensional shrinking of the nanofibers and keeping the tight-pulled mat confined within the frames during the crosslinking process. Afterwards, supplementary frames were mounted on the reverse side in order to fix firmly the crosslinked nanofiber mats for the following steps.

2.3.3.2. Composite membrane of SPEEK-35PVA reinforced with SPEEK-30PVB nanofibers

A water-based solution of SPEEK-35PVA (7.5 wt% concentration) was used for infiltration within the nanofibers. In this method, the nanofibers were immersed in the cited solution for 5 minutes and then placed in a climate chamber (INELTEC CCSR-0/50, Spain)

at 90°C with a low humidity level for another 5 minutes. This process was repeated 4 times rotating the nanofiber mat 90° angle in each step. In the final step, the mat was left in the climate chamber during 10 minutes to enhance the drying of the composite membrane that was prepared. Then, the membranes were cut along the borders of the frames and left at room temperature overnight to ensure total dryness.

Finally, square membranes (5x5 cm²) were cut and crosslinked at 120°C for 1 hour under a pressure of 1 kN cm⁻² by applying the hot plate press (Rondol). Similarly, the prepared composite membranes were boiled in water for 1 hour and stored in water at room temperature.

2.4. Characterization of membranes

2.4.1. Water uptake and ion-exchange capacity (IEC)

Water uptake was calculated based on the difference in weight between the wet and dry membranes, according to the following expression,

$$\text{Water uptake (\%)} = \frac{m_{\text{wett}} - m_{\text{dry}}}{m_{\text{dry}}} \times 100 \quad (1)$$

Since there was some solubility of the polymer from the membranes during treatment in boiling water, the blend membranes were weighed after keeping them for 1 hour in boiling water (m_{wet}), and after 3 hours in an oven at 100°C, followed by another 3 hours in vacuum at the same temperature (m_{dry}). This operation was repeated three times in order to get an average value. In Table 1, we report the values of water uptake for the membranes used in this study.

For the ion-exchange capacity (IEC), as-prepared proton form membranes, previously swollen in water, were immersed in 50 ml of 2 M NaCl solution for 1 day. Afterwards, the solution was titrated with 0.01 M NaOH against a Phenolphthalein indicator and the IEC calculated from the following equation:

$$\text{IEC (meg/g)} = \frac{V_{\text{NaOH}} \times 0.01}{m_{\text{dry}}} \quad (2)$$

where V_{NaOH} is the volume of NaOH solution used during the titration (ml) and m_{dry} the weight of the membrane immersed in the solution after being dried (grams). The pertinent results of the *IEC* values are also given in Table 1.

2.5. Oxygen permeability (electrochemical method)

The diffusion characteristics of the membranes were determined by utilizing the experimental assembly commonly used to measure the permeability of oxygen through contact lenses, described elsewhere [25]. Briefly, it comprises a permeometer (Rheder Development Co., model 201 T) in which the polarographic cell is a solid cylindrical cathode of gold carat (4.25 mm diameter and 6 mm long). The anode is a silver hollow cylinder 7 mm long, the inner and outer diameters being 5 and 10 mm, respectively. More details and a sketch of the experimental assembly are given in several papers [25-27].

The oxygen permeates from one side of the membrane, where the partial pressure of the gas is kept constant ($p = p_L = 155$ mm Hg), to the other side, facing the cathode of the polarographic cell, where the partial pressure is $p_0 = 0$. The oxygen flux through the hydrogel is determined from the measurement of the electric current density, with a potentiostat coupled to the permeometer. The cathode is maintained at -0.75 V with respect to the silver anode. All the oxygen passing through the sample is reduced at the cathode. In steady state conditions ($t \rightarrow \infty$), the current intensity can be written as, [25]

$$I_{\infty} = \frac{nFADk p_L}{L_{\text{av}}} \quad (3)$$

while the apparent transmissibility, T_0 , is calculated as,

$$T_0 = \frac{Dk}{L_{\text{av}}} = \frac{1}{nAF p_L} I_{\infty} = B I_{\infty} \quad (4)$$

and finally, the apparent permeability ($P=Dk$) is given by,

$$P = Dk = \frac{L}{nAF p_L} I_{\infty} \quad (5)$$

where D and k are the diffusion coefficient and Henry's law of solubility constant, respectively, L_{av} is the thickness of the membrane, I_{∞} is the steady-state current intensity, n (=4) the number of electrons exchanged in the electrodes for each molecule of oxygen reduced, A is the surface area of the cathode in contact with the polymer sample, F is Faraday constant (= 96487 C/mol vol O₂ (STP) = 96487A s/22400 cm³ O₂ (STP)), p_L the O₂ partial pressure difference across the hydrogel (155 mmHg) and B is a constant for the cell in the given conditions, in this case $B = 0.02629$ cm³ of O₂(STP) cm⁻² s⁻¹cmHg⁻¹. The measurements were carried out by dissolving atmospheric oxygen in water, later replacing the membrane and then, the amount of oxygen diffused through the membrane was monitored at the cathode, where the reduction took place. Prior to the measurements, the membranes were swollen in water until equilibrium was attained.

2.6. Membrane conductivity measurements (impedance analysis)

Impedance measurements were carried out on the membranes at 25°C and a frequency (f) window $10^{-1} < f < 10^7$ Hz. The experiments were performed with 100 mV amplitude waves, using a Novocontrol broadband dielectric spectrometer (Hundsangen, Germany) integrated to an SR 830 lock-in amplifier with an Alpha dielectric interface. The membrane were previously equilibrated with water and afterwards was sandwiched between two circular gold electrodes in a liquid parallel plate cell coupled to the spectrometer acting as blocking electrodes and incorporating deionized water (Milli-Q) to ensure fully hydrated state of the membranes. During the conductivity measurements, the temperature was controlled by a nitrogen jet (QUATRO from Novocontrol) with a temperature variation of 0.1 K during every single sweep in frequency. Each measurement was repeated four times to assure the reproducibility of the measurements.

Traditionally, the equivalent circuit describing the response of a proton-conducting membrane to an alternating electric field, consists of a resistance R_0 that accounts for proton resistance in the membrane in circuit series, made up of a resistance R_p (representing a polarization resistance) in parallel with a constant phase element (CPE) of admittance $Y^*=Y_0(j\omega\tau)^n$ ($0 < n \leq 1$). This CPE accounts for the interfacial phenomena in the membrane-electrode interface. The impedance circuit is given by, [28]

$$Z^* = R_0 + \frac{R_p}{1 + R_p Y_0 (j\omega\tau)^n} \quad (6)$$

where ω is the angular frequency and τ is the relaxation time. The plot of the imaginary part Z'' vs the real part Z' of equation 6, called a Nyquist diagram [29], is a semicircle that intersects the abscissa axis at $Z' = R_0$ and $Z' = R_0 + R_p$ in the extreme values of frequency $\omega \rightarrow \infty$ and $\omega \rightarrow 0$, respectively. An alternative plot that is used here consists of the Bode diagram [30]. In this case, the frequency dependence of the complex impedance, $|Z^*|$, decreases from R_p at $\omega \rightarrow 0$ to R_0 at $\omega \rightarrow \infty$. Moreover, the out of phase angle $\phi = \tan^{-1}(Z''/Z')$ increases with increasing frequency, reaching a maximum ($\phi = 0$) at $\omega \rightarrow \infty$. The resistance R_0 was taken as the value of $|Z^*|$ at the frequency at which $\phi = 0$. The conductivity of the membranes were calculated from the resistances obtained from the Bode diagrams by means of the expression,

$$\sigma = \frac{l}{R_0 S} \quad (7)$$

where σ , S and l are the proton conductivity, area and thickness of the membrane in contact with the blocking electrodes, respectively.

2.7. Sampling and electrochemical (E) method of enrichment of inoculum

Samples were collected according to the procedure described previously by the authors [6] from the former Texcoco lake in a sterile anaerobic container and preserved aseptically. The sampling site is the dry bottom of a historically desiccated lake in central Mexico; the salts were accumulated in the process of desiccation, and the soils are known to be saline-sodic. Moreover, very few studies had been investigated with respect to the role of saline biocatalyst in anode, as well as it had more attraction in the field of novel osmosis process for wastewater treatment process [26]. A Texcoco soil bacterial inoculum was enriched and preserved in modified Soap Lake basal medium (SLBM) called SL3 medium [27] which contains 20 mM of sodium acetate as carbon source. This medium was used for the enrichment, preservation and electrolysis processes. The culture was thermally isolated to preserve the medium at +4°C. The electrochemical enrichment was performed through

an electrolysis process using graphite as a working and counter electrodes, applying a potential of -150 mV over 150 days [31-33]. The procedure was repeated twice at which point hybrid H inocula was finally obtained. A schematic representation of the process followed from the sodic saline soil until the formation of the hybrid H-inocula is given in Figure 1. This Hybrid inoculum was used in MFCs as a biocatalyst (1 g of wet weight) in the anode and model high concentrated sodic saline waste water as SL3 medium.

2.8. Most probable number (MPN) of iron reducing bacteria

The most probable number (MPN) was measured following the same steps shown in a recent paper published by a part of the authors [6]. Briefly, an amount of 1 g of biofilm scraped from the bio-electrolysis cell was transferred into 99 mL of modified SL3 medium containing 15 mM of sodium acetate used as carbon source and 100 mM iron (III) citrate as terminal electron acceptor. Afterwards, a 10 mL volume of the above inoculum solution was transferred into 90 mL of SL3 medium (first 1:10 serial dilution), from which 10 mL of inoculum solution was transferred again into 90 mL of SL3 medium (1:100 dilution). Similarly, the process was repeated up to a 10^{-4} dilution. Each transfer was incubated for 12 days. At the end of each transfer, the iron(II) concentration was detected as the positive end-point using the ferrocine technique [34].

2.9. Molecular Characterization of Hybrid-H inocula

A DNA sample of the 'Hybrid-H' was extracted using an UltraClean soil DNA isolation kit (MO BIO Laboratories, Solana Beach, CA) according to the manufacturer's instructions. Primers 27F and 1392R were used to amplify a variable region of the bacterial 16S rRNA gene [35,36]. Archaea primers 21F and 1392r were used to amplify a variable region of the 16S rRNA gene [35]. The PCR products were visualized by agarose gel electrophoresis 1% (w/v) with ethidium bromide staining. PCR amplification products were purified using a QIAquick PCR purification kit (Qiagen, Valencia, CA, USA). PCR products were cloned directly into the vector pCR-XL-TOPO cloning kit (Invitrogen Life Technologies, Carlsbad, CA, USA). The manufacturer's protocol was followed throughout the cloning process including chemical transformation. Plasmid DNA was isolated from the clone-cultures using a miniprep plasmid extraction method [37] to test for the presence of

insert fragment gene on the plasmids under the above-described conditions. Plasmids were digested with EcoR1 restriction enzymes to detect the insertion (Sigma-Aldrich) according to the manufacturer's instructions. The digestion patterns were viewed on a 1% agarose gel. The 16S rRNA sequences were obtained with an ABI PRISM 310 Genetic Analyzer (Applied Biosystems, Foster City, CA, USA) using M13 primers. Molecular identification was carried out using BLAST search. (Gene Bank Access Numbers as follows KF952451 - 53 and KF952481 -84).

2.10. Construction of single chamber microbial fuel cell

Details of the design and construction of a single chamber microbial fuel cell (SCMFC) can be found elsewhere [33]. In summary, the MFC consisted of a vertical cylinder built in glass, 9 cm long and 5.6 cm internal diameter (200 mL capacity). Nafion® 117 was treated by consecutive boiling processes for 1h in 3% H₂O₂, 2M H₂SO₄ and deionized water, according to the procedure previously described [38,39]. The other composite membranes were pre-treated with hot distilled water (60°C) for 30 minutes, before spraying the catalyst; all the membranes were dried and flattened. Later on, an oxygen reduction active layer was sprayed with a catalyst loading of 0.5 mg cm⁻² Pt (10 wt%/C-ETEK), followed by hot-pressing of the membranes at 120°C and 11 kg cm⁻² for 1 min. An assembly of anode-proton exchange membrane-cathode (AMC) was fitted at the bottom of the cell. The AMC, in turn, consisted of (from top to bottom) a perforated stainless steel plate (1 mm thick current collector), a Toray flexible carbon cloth sheet (23 cm² anode electrode), a proton exchange membranes Nafion-117, Nafion-PVA-15, Nafion-PVA-23, SPEEK-35PVA(Water), SPEEK-35PVA(DMAc) and SPEEK-PVA-PVB each was used. An oxygen reduction active catalyst layer was applied with a catalyst loading of 0.5 mg cm⁻² Pt (10 wt%/C-ETEK), followed by a cathode made of Toray flexible carbon cloth, and a perforated plate of stainless steel as current collector (1 mm thick) [33].

2.11. Electrochemical characterization of microbial fuel cells

The membranes prepared in this work (blended- and nanocomposite-type) and a commercial Nafion-117 membrane were fitted in single chamber microbial fuel cells and characterized by linear sweep voltammetry (LSV) and electrochemical impedance

spectroscopy (EIS). Linear sweep voltammetry (LSV) was performed in a Potentiostat/Galvanostat PARSTAT 2273, run at a recommended scan rate of 0.1 mV s^{-1} , starting from the measured open circuit potential up to +50 mV [40-42]. Impedance spectra of microbial fuel cells were obtained at the open circuit potential (E_{ocp}). The amplitude of the signal perturbation was 10 mV, scanned in the frequency range from 100 kHz to 1 mHz. Data fitting was accomplished by Z-view software.

3. Results and Discussion

3.1. Characterization of membranes

The technique described by Aiba et al. 1968 [43] to determine the oxygen transport coefficients in polymeric membranes was used. This method permits the measurement of the apparent oxygen transmissibility and, separately, the transport coefficients in the case of hydrogel contact lenses [25,44-48]. By means of the apparatus used in this study (permeometer model 201T from Rheder Development Co.), commonly used in experimental measurements, we can conclude from results reported in Table 2 that incorporation of PVA nanofibers into a Nafion® matrix (Nafion-PVA-15 and Nafion-PVA-23) strongly restricts permeation of oxygen in comparison with the pristine polymer (Nafion-117). Similarly, we can see that membranes based on SPEEK have an oxygen permeability one order of magnitude smaller than Nafion-117 membranes. The barrier effect of the crosslinked PVA nanofiber phase, together with the constrained swelling of the Nafion® matrix and SPEEK based, produce a reduction of the oxygen permeability through Nafion-PVA and SPEEK-30PVB-35PVA that can lead to good results when these membranes have to be applied in MFC's.

The experimental results of apparent transmissibility and permeability are given in Table 2.

From Table 2, the apparent oxygen transmissibility of the membranes follows the following order: Nafion-117 > Nafion-PVA-15 > Nafion-PVA-23 > SPEEK-30PVB-35PVA > SPEEK-35PVA (Water) > SPEEK-35PVA(DMAc). Interestingly, the nanocomposite membranes of Nafion-PVA-15 and Nafion-PVA-23 showed lesser oxygen transmissibility than the commercial Nafion-117, typically considered for MFC application. SPEEK35PVA(DMAc) showed the lowest oxygen permeability among the membranes

studied. The order of the different membranes according to the oxygen permeability is as follows: Nafion-117 > SPEEK-30PVB-35PVA = SPEEK-35PVA(Water) > Nafion-PVA-23 > Nafion-PVA-15 > SPEEK-35PVA(DMAc). We can conclude from Table 2 that incorporation of PVA nanofibers into a Nafion® matrix (Nafion-PVA-15 and Nafion-PVA-23) strongly restricts permeation of oxygen in comparison with the pristine polymer (Nafion-117). The barrier effect of the crosslinked PVA nanofiber phase, together with the constrained swelling of the Nafion® matrix, would explain the observed results in terms of the mechanical reinforcement provided by the nanofibers.

A close comparison between the SPEEK-based membranes emphasizes the effect of the solvent in the membrane properties to achieve lower oxygen permeation than water. The SPEEK-based membranes prepared using water as solvent present similar values of oxygen permeability, thus indicating that the SPEEK-30PVB nanofibers do not cause any improvement in the properties of the membrane in this case. It might be expected for the PVB phase in the nanofibers to have a smaller barrier effect towards oxygen transportation than PVA, due to the amorphous structure of the former as the butyral side chains impede packing of the polymer backbones. On the other hand, PVA is a crystalline polymer with strong hydrogen-bonding between chains (due to the OH groups), consequently, a high ordering of the polymer chains usually takes place, and good barrier properties can be expected in PVA as confirmed from our results. The calculated values of electrical conductivity are shown in Table 3.

When fuel cell data are not available, prediction of the fuel cell performance is often made using the so-called characteristic number of a specific membrane, defined by the ratio between the proton conductivity of the membrane and its methanol permeability [49, 50], $\beta = \sigma/P$. Using the same concept as in DMFC, we can define this parameter for MFCs as the ratio of the proton conductivity of the membrane to its oxygen permeability. The values obtained for our membranes are also given in Table 3. Evaluation of this β parameter is important, because it is independent from the membrane thickness [49]. Membranes can be ordered as a function of their descending β values (Table 3) as follows: SPEEK-30PVB-35PVA > Nafion-PVA-15 > Nafion-PVA-23 > SPEEK-30PVA(DMAc) > SPEEK-35PVA(Water) > Nafion-117. Interestingly, the composite membranes containing nanofibers exhibited the best characteristic numbers in comparison with the blended

membranes and commercial Nafion-117. This property is very attractive when it is used in MFCs, since those membranes will give strict anaerobic condition in the anodic chamber as well as good proton conductivity, thus enhancing the cathodic activity. In comparison with Nafion-117, the nanofiber-reinforced membranes show β values about three times larger.

3.2. Characterization of inocula

The scanning electron micrograph (SEM) of the hybrid inoculum on the anodic carbon cloth surface is shown in Fig. 2. The presence of microbial colonies along with the bacterial nanowires on the surface can easily be inferred. Interestingly, the physical structural features of the *Geobacter* species with bacterial nanowire, further confirmed as *Geobacter metallireducens* by the molecular biology techniques. Unexpectedly, MPN of Fe(III)-reducing bacteria was reduced to about 45% from the initial amount in the last transfer during the enrichment processes (Table S1). Electrochemical activity of the Hybrid inoculum on the anodic carbon cloth is shown in Fig. 3. The bare carbon cloth did not show any electrochemical response; we can conclude that there is no current generation in the absence of microflora in the SCMFC. The biofilm that was formed on carbon cloth exhibited two redox reactions on the surface with midpoint potentials of -385 mV and +18 mV vs SCE, respectively. The midpoint potential of -385 mV might be associated with membrane bound enzymes of the sodic-saline micro-flora, in accordance with previously reported results [51], whereas the potential +18 mV/SCE could be associated to the soluble cytochrome activity, in accordance with the results of Tomlinson et al. [52].

In the enriched 'hybrid-H' inocula, 67 % of the sequences obtained in the 16S rDNA clone library were Delta proteobacteria. The genus of *Desulfurivibrio alkaliphilus*, and *Geobacter metallireducens* were sharing the equal abundance (33%) (Table 4). The other bacteria class was Gamma proteobacteria (33%). The genus is *Marinobacter adhaerens* (33% of abundance).

The power production led to the hybrid H inocula in the anode and it exhibits the relative abundance of the Delta proteobacteria (Table 4). *Geobacter metallireducens* familiar for their electrochemical activity in MFCs have been found enriched in the 'hybrid-H', recent report also coherence with activity in high salt concentrations [53]. Indeed, in extreme haloalkalophile *Desulfurivibrio alkaliphilus*, which is a sulfate reducing bacteria

commonly found in soda lakes [54], Interestingly, *Desulfurivibrio alkaliphilus* is also found in long rang electron transfer through filaments, in which its activity might be employed to form an electrochemical activity in MFC [55]. Recently, *Marinobacter adhaerens* is known for their electrochemical activity on copper alloy [56].

The archaea clones from the ‘hybrid-H’ could belong to the group of Methanococci (100%) with the most dominant groups being *Methanocaldococcus infernus* (75% of abundances) (Table 4). Partial flux of electrons through the anaerobic food chain to methanogenesis may support a normal anaerobic community and respiratory organisms [57]. Thus, it is not surprising that such surveys find a general enrichment of syntrophic organisms such as many Proteobacteria. Consequently, the metal-reduction machinery was well-suited for harvesting the electrochemically active inocula [58].

3.3. In-situ characterization of reinforced membrane in single chamber microbial fuel cells

We characterized the different proton exchange membranes in single chamber microbial fuel cells (SCMFCs) using electrochemically enriched sodic saline inocula as biocatalyst (910 mW/m³) [6]. Electrochemical polarization curves of the SCMFCs are shown in Fig 4a. Results of the performance curves of Fig 4b conducted to a maximum power density of 1053 mW/m³ at a voltage of 0.340 V on Nafion-PVA-15. Results on Nafion-117, Nafion-PVA-23, SPEEK-PVA-PVB, SPEEK-35PVA(Water) and SPEEK-35PVA(DMAc) are described in Table 5. The decrease observed in voltage, current and power density of the polarization curves could be associated to biofilm formation by bacteria on the anode and planktonic bacteria in bulk solution or to inherent electrochemical electron transfer kinetics and mass transport within the supported catalyst inherent layers, because the activity in the membrane assembly could be influenced by its particle size, surface morphology and support structure, recognizing as having an influence on the electricity generating bacteria of the microbial fuel cell. [59]

One of the main challenges in the MFCs is reducing as much as possible the internal resistance due to separators such as proton exchange membranes, in order to obtain a higher performance and power density. For this reason a great number of studies have been focused on the EIS applied to MFC [60-62]. In this way we know that the use of metallic current collectors pressed against the electrodes, permit to reduce the R_{int} of the system

[63], although this is not the case that we have studied. As indicated above is the impedance response observed for each electrode-electrolyte interfaces which reveals a frequency dispersion of the electrical properties of the interface produced onto the material [28]. There are two ways to shown the results observed in EIS. The Nyquist [29] diagram where the negative imaginary part of the complex impedance ($-Z''$) is plotted versus the real part of the impedance (Z'), and the Bode [30] plot. Nyquist diagrams obscure the frequency dependence because this magnitude is not made explicit in such plots. The Bode plot is more sensitive to characterize the system parameters when we compare models with experimental data [64]. Usually, the equivalent circuit describes the response of a proton-conducting membrane to an alternating electric field. In our study we are used the same equivalent circuit that who has been employed by Liang et al [65] and such as shown in the inset of figure 5, which consists of a resistance R_0 that accounts for proton resistance in the membrane in circuit series between two circuits made up of a resistance $R_{p,i}$ (i for anode and cathode, respectively) representing a polarization resistance in parallel, each one, with a constant phase element (CPE), characteristic of anode and cathode electrical double layer capacitance, respectively, figure (5).

The experimental results together with the theoretical model corresponding to the equivalent circuit used are given in figure 5, where the symbols represent the experimental data and the line the modeled fit. In our study we have characterized two different proton exchange membranes using the single chamber microbial fuel cells (SCMFC) described above with electrochemically enriched sodic saline inocula as biocatalyst [6]. A type of proton exchange membranes are, composite membranes based on poly(ether ether ketone) (SPEEK) and, the other hand, Nafion® reinforced with PVA nanofibers. From the fits we are obtained the values of $R_{p,a}$, $R_{p,b}$ and $R_{memb+sol}$, respectively. These values are given in table 5. A comparison between the PEM based Nafion® revealed that the Nafion-PVA-15 composite membrane presents the lowest total internal resistance, just reaching a value of $522.0 \pm 0.9 \Omega$ and exhibit the low $R_{memb+Ohm}$, of $0.5 \pm 0.7 \Omega$, in agreement with the low oxygen permeability that have this kind of membranes. On the other hand the combination of permeability and conductivity given by the evaluation of β parameter of table 3, We could consider that the membrane Nafion-PVA will pave the way to attain the maximum power density ($1053 \text{ mW/m}^3 / 91 \text{ mW/m}^2$) in SCMFCs (Table 5.). Our results show that power

density by Nafion-PVA was superior to other composite membrane, reaching the highest power density established recently by high saline MFCs system. Some authors have obtained very interesting results for high saline MFCs. Miller and Oremland 2008 reported 18.5 mW/m² for Mono lake sediment (with the presence of exoelectrogens for efficient electron transfer) [66]. Also a maximum of current density of 12.5 mA/m² for Soap Lake inocula with in dual chamber MFC had been reported [67]. Slightly higher power density had been reported for *H. volcanii* (509.8 mW/m²) [68]. However, they provide the neutral red as mediator with ferricyanide as cathode, made as unfavorable for the MFCs field operation, due to toxicity/instability of mediators and environmental issues [69].

Furthermore, in Table 6, our results are compared to the other composite membrane with air cathodic MFCs system published by other authors. Although our composite membrane could be comparable concerning their power density with other MFCs design (Table 6), several critical factors (geometrical design, electrode-membrane ratio, etc.) forbid a direct comparison with other published data. Moreover, when comparisons are made using the results obtained in this work, by means of the same air cathodic MFCs, valid conclusion can be elaborated. Remarkably, we didn't provide any additional input energy (agitation, circulation, and/or air purging).

Composite membrane based on SPEEK fitted SCMFC showed the EIS value in table 5. It follows the tendency of SPEEK-PVA-PVB < SPEEK-35PVA(Water) < SPEEK-35PVA(DMAc) in $R_{\text{memb+Ohm}}$. In composite membrane of SPEEK incorporation of PVA and PVB displayed low $R_{\text{memb+Ohm}}$. Unexpectedly, this order also follows in SCMFC performance, even though it has low β parameter.

The comparison between the reinforced Nafion membranes with PVA and Nafion®117 show that MFCs performance present the following trend: Nafion-PVA-15 > Nafion-117 > Nafion-PVA-23. Nafion incorporation with PVA 15 membrane exhibited the very low ohmic resistance that we could conclude from the Polarization Curve and EIS. (Fig. 4 and 5). This could favor the ion transport through the Nafion PVA 15 composite membrane and reduce the membrane resistance. As a result of this, it could be the better alternative composite membrane. While if we compare the composite membranes based on SPEEK the results are: SPEEK-PVA-PVB > SPEEK-35PVA(Water) > SPEEK-35PVA(DMAc). Composite membrane of SPEEK-PVA-PVB revealed less ohmic

resistance (Fig. 4 and 5) than the SPEEK composite membrane. Comparison of ex-situ results of MFCs performance against the in-situ membrane characterization in SCMFCs shows some mismatch between the expected behaviors and the ones actually observed. An explanation may be given in terms of the mechanical stresses induced in the membranes during their assembly with the electrodes (MEAs) through the hot press method, which may have affected membrane properties and thus the final MFC performance [70-72]. Another reason might be that the usual binder of the catalyst particles on the electrodes is a Nafion® ionomer, and therefore, the compatibility/adhesion of the electrodes with the Nafion-based membranes is expected to be higher than it is in cases of non-Nafion membranes, as those composed of SPEEK [73,74].

In this sense, the nanocomposite membrane of Nafion-PVA-15 exhibited the best performance inside the SCMFCs (in-situ) as well as good ex-situ results. Therefore, this membrane will be the most suitable choice for saline wastewater MFC applications.

3.4. Batch Operation of Nafion PVA-15 and Nafion 117

We selected the highest performance of two Nafion based composite membranes (Nafion-PVA 15 and Nafion 117) in SCMFC were fitted with batch operation at 450 hrs, employing synthetic high concentration of sodic saline wastewater as source and electrochemically active sodic-saline inocula as biocatalyst in anode. Batch operation were performed by applying of $1k\Omega$ resistance to SCMFC, after the SCMFC reached steady state condition (OCP around 640 mV) in 6 hrs. In both case, after applying the external resistance to SCMFC, gradually increase the potential (Fig. 6) and attain plateau region. Nafion based composite membrane Nafion-PVA 15 attained the plateau region around 410 mV and maintained at 150 hrs. Nafion-PVA 15 presented the columbic efficiency (η_{Coul}) of 12 % and average volumetric power density of 434 mW/m^3 at average potential of 274 mV. Commercial Nafion-117 membrane revealed the short plateau region around 309 mV for 63 hrs. Later on gradually decreases with time. Nafion-117 revealed the columbic efficiency (η_{Coul}) of 10 % and average volumetric power density of 262 mW/m^3 at potential (average) of 206 mV. The batch operation was ended at 450 hrs. Further, we analyzed the EDAX results of before (supporting information Fig 1.) and after the SCMFC (Fig 7.). We found the presence of trace amount cations, such as Na, Ca, Mg and Mn, on the Nafion-117 after

the SCMFC performance. This could be the possible reason of short plateau region, responsible for hindering the cathodic reaction and decrease the performances of Nafion-117 in SCMFC. This also, would be speculated that the stability of the Nafion-117 under synthetic high concentrated sodic-saline wastewater may be deprived. Up to now, very limited information is available for the high concentration of sodic-saline wastewater treatment in MFC. Subsequently, low loading rate of Nafion reinforced composite membrane could be the better candidate for high concentrated sodic-saline wastewater treatment through SCMFC.

The polarization curves in region of the MFC operation, i.e., the activation and ohmic region of fig 3, was analyzed by applying the relationship between the external voltage and current, where a maximum power density described by eq.(8) [75] was obtained:

$$P_{\max} = 0.45 \frac{E_b^2}{R_{\text{int}}} \quad (8)$$

The maximum power density is the quadratic function derived from the lineal polarization voltage intercept (E_b) and the total internal resistance R_{int} of the MFC, deduced from the linear slope of polarization curves. Table 6 summarizes values of volumetric power density and compared with results reported in literature. Interestingly nanofiber based composite membrane exhibit superior characteristic with saline inocula. Results of polarization curves are in agreement with that obtained with EIS analysis and superior reported in literature.

4. Conclusions

The membranes were characterized in single chamber microbial fuel cells (SCMFCs) using electrochemically enriched high sodic saline hybrid H-inocula (67% of the sequences obtained in the 16S rDNA clone library were Delta proteobacteria). The genus of *Desulfurivibrio alkaliphilus*, and *Geobacter metallireducen* were sharing the equal abundance (33%)) as biocatalyst. The results show that Nafion-PVA-15 provided a maximum power density of 1053 mW/m³ at a voltage of 340 mV, which was superior to the behavior obtained with commercial Nafion-117, and with the lab-prepared Nafion-PVA-23, SPEEK-35PVA(Water), SPEEK-35PVA(DMAc) and SPEEK-PVA-PVB

membranes. Electrochemical impedance spectroscopy characterization revealed a lower total internal resistance ($R_{int}=522 \Omega$) on Nafion-PVA-15 in comparison with the other membranes. The reason behind the superior performance of Nafion-PVA-15 might come from the ultrathin thickness (reduced ohmic resistance) and its high characteristic number (β) and low oxygen permeability value, resulting from the introduction of crosslinked PVA nanofibers into the Nafion® matrix. Results of this study are encouraging towards the procurement of a cost effective and optimized high concentrated sodic saline model wastewater exploiting MFCs.

Acknowledgements

The authors wish to thank SEP and CINVESTAV-IPN for granting a PhD fellowship to one of the authors (KSK). We gratefully acknowledge the financial support of the National Council of Science and Technology, CONACYT, under grant FOINS 75/2012 and the Ministry of Science and Innovation of Spain through the project SP-ENE-20120718 and Support Programme for Research and Development of the Polytechnic University of Valencia through the project ref. 24761. Dr O. Solorza thanks Plan de Movilidad e Internalización Académica VLC/CAMPUS fellowship at the Universidad Politécnica de Valencia.

References

- [1] Ghadge AN, Ghangrekar MM. Development of low cost ceramic separator using mineral cation exchanger to enhance performance of microbial fuel cells. *Electrochimica Acta* 2015; 166: 320-326.
- [2] Sciarria TP, Merlino G, Scaglia B, D'Epifanio A, Mecheri B, Borin S, Licoccia S, Adani F. Electricity generation using white and red wine lees in air cathode microbial fuel cells. *Journal of Power Sources* 2015; 274: 393-399.
- [3] Sharma M, Bajracharya S, Gildemyn S, Patil SA., Alvarez-Gallego Y, Pant D, Rabaey K, Dominguez-Benetton X. A critical revisit of the key parameters used to describe microbial electrochemical systems. *Electrochimica Acta* 2014; 140: 191-208.

- [4] Molognoni D, Puig S, Balaguer MD, Liberale A, Capodaglio AG, Callegari A, Colprim J. Reducing start-up time and minimizing energy losses of Microbial Fuel Cells using Maximum Power Point Tracking strategy. *Journal of Power Sources* 2014; 269: 403-411.
- [5] Li Y, Wu Y, Puranik S, Lei Y, Vadas T, Li B. Metals as electron acceptors in single-chamber microbial fuel cells. *Journal of Power Sources* 2014; 269: 430-439.
- [6] Sathish-Kumar K, Solorza-Feria O, Tapia-Ramírez J, Rinderknecht-Seijas N, Poggi-Varaldo HM. Electrochemical and chemical enrichment method of a sodic-saline inoculum for microbial fuel cells. *Int. J. Hydrogen Energy* 2013; 38: 12600–12609.
- [7] Dominguez-Benetton X, Sevda S, Vanbroekhoven K, Pant D. The accurate use of impedance analysis to the study of microbial electrochemical systems. *Chem. Soc. Reviews* 2012; 41:7228-7246.
- [8] Schröder U. From in vitro to in vivo—biofuel cells are maturing. *Angew. Chem. Inter. Edition* 2012; 51: 7370-7372.
- [9] Pant D, Van Bogaert G, De Smet M, Diels L, Vanbroekhoven K. Use of novel permeable membrane and air cathodes in acetate microbial fuel cells. *Electrochim. Acta* 2010; 55: 7710-7716.
- [10] Liu H, Cheng S, Logan BE. Power Generation in Fed-Batch Microbial Fuel Cells as a Function of Ionic Strength, Temperature, and Reactor Configuration. *Environ. Sci. Technol* 2005; 39: 5488-5493.
- [11] Kim JR, Min B, Logan BE. Evaluation of procedures to acclimate a microbial fuel cell for electricity production. *Appl. Microbiol. Biotechnol.* 2005; 68: 23-30.
- [12] Logan BE, Murano C, Scott K, Gray ND, Head IM. Electricity generation from cysteine in a microbial fuel cell. *Water Research* 2005; 39: 942-952.
- [13] Zhang X, He W, Ren L, Stager J, Evans PD, Logan BE. COD removal characteristics of air-cathode microbial fuel cells. *Biores. Technol* 2015; 176: 23-31.
- [14] Mauritz KA, Moore RB. State of Understanding of Nafion. *Chem. Rev* 2004; 104: 4535-4585.
- [15] Rozendal RA, HamelersHVM, Buisman CJN. Effects of membrane cation transport on pH and microbial fuel cell performance. *Environ Sci Technol.* 2006; 40: 5206-5211.

- [16] Aldrovandi A, Marsili E, Stante L, Paganin P, Tabacchioni S, Giordano A. Sustainable power production in a membrane-less and mediator-less synthetic wastewater microbial fuel cell. *Bioresource Technology* 2009; 100: 3252-60.
- [17] You S, Zhao Q, Zhang J, Jiang J, Wan C, Du MA. A graphite-granule membrane-less tubular air-cathode microbial fuel cell for power generation under continuously operational conditions. *Journal Power Sources* 2007; 173: 172-177.
- [18] Zhu N, Chen X, Zhang T, Wu P, Li P, Wu J. Improved performance of membrane free single-chamber air-cathode microbial fuel cells with nitric acid and ethylenediamine surface modified activated carbon fiber felt anodes. *Bioresource Technology* 2011; 102: 422-426.
- [19] Mollá Sergio, Compañ Vicente, Polyvinyl alcohol nanofiber reinforced Nafion membranes for fuel cell applications. *J. Membrane Science* 2011; 372: 191-200.
- [20] Mollá Sergio, Compañ Vicente. Novel ultrathin composite membranes of Nafion/PVA for PEMFCs. *Int. J. Hydrogen Energy* 2011; 36: 9886-9895.
- [21] Mollá, Sergio, Compañ Vicente. Performance of composite Nafion/PVA membranes for direct methanol fuel cells. *Journal of Power Sources*, 2011;196:2699-2708.
- [22] Carbone A, Pedicini R, Portale G, Longo A, D'Ilario L, Passalacqua E. Sulphonated poly(ether ether ketone) membranes for fuel cell application: thermal and structural characterisation. *J Power Sources* 2006;163:18-26.
- [23] Knauth P, Hou H, Bloch E, Sgreccia E, Di Vona ML. Thermogravimetric analysis of SPEEK membranes: thermal stability, degree of sulfonation and cross-linking reaction. *J Anal Appl Pyrolysis* 2011;92:361e5.
- [24] Mollá Sergio, Compañ Vicente. Polymer blends of SPEEK for DMFC application at intermediate temperatures. *Int. J. Hydrogen Energy* 2014; 39: 5121-5136.
- [25] Compañ V, Tiemblo P, García F, Garcia JM, Guzmán J, Riande EA. A potentiostatic study of oxygen transport through poly(2-ethoxyethyl methacrylate-co-2,3-dihydroxypropylmethacrylate) hydrogel membranes. *Biomaterials* 2005; 26: 3783–3791.
- [26] Zhang, Fei; Kristen S. Brastad and Zhen He. Integrating Forward Osmosis into Microbial Fuel Cells for Wastewater Treatment, Water Extraction and Bioelectricity Generation. *Environ.sci.techno*2011; 45(15), 6690-96.

- [27] Mormile MR, Romine MF, Garcia MT, Ventosa A, Bailey TJ, Peyton BM. *Halomonas campisalis* sp.nov., a Denitrifying, Moderately Haloalkaliphilic Bacterium. *Systematic and Applied Microbiology* 1999; 22: 551-558.
- [28] Evgenij B, Ross Macdonald J. Impedance spectroscopy: Theory, Experiment and Application, Chap. 2, 2005; pp 87-88, Wiley-Interscience, Chichester.
- [29] Nyquist H. Thermal agitation of electric charge in conductors. *Phys. Rev* 1928; 32:110-113.
- [30] Bode WW. Network Analysis and Feedback Amplifier Design, Van Nostrand, Princeton, NJ., 1956.
- [31] Aelterman P, Freguia S, Keller J, Verstraete W, Rabaey K. The anode potential regulates bacterial activity in microbial fuel cells. *Applied Microbiology Biotechnology* 2008; 78: 409-18.
- [32] Torres CSI, Krajmalnik-Brown R, Parameswaran P, Marcus AK, Wanger G, Gorby YA. Selecting Anode-Respiring Bacteria Based on Anode Potential: Phylogenetic, Electrochemical, and Microscopic Characterization. *Environmental Science & Technology* 2009; 43: 9519-9524.
- [33] Sathish-Kumar K, Solorza-Feria O, Vázquez-Huerta G, Luna-Arias JP, Poggi-Varaldo HM. Electrical stress-directed evolution of biocatalysts community sampled from a sodic-saline soil for microbial fuel cells. *J. New Mat. Electrochem. Systems* 2012; 15: 181-186.
- [34] Lovley DR, Phillips EJ. Novel mode of microbial energy metabolism: organic carbon oxidation coupled to dissimilatory reduction of iron or manganese. *Applied and Environmental Microbiology* 1988; 54(6): 1472-1480.
- [35] Lane DJ. 16S/23S rRNA sequencing, In E. Stackebrandt, and M. Goodfellow (ed.), *Nucleic acid techniques in bacterial systematics*. John Wiley and Sons, 1991, p. 115-175.
- [36] Stahl DA, Amann R. *Nucleic acid techniques in bacterial systematics*, eds E. Stackebrandt and M. Goodfellow. Wiley, Chichester, England. New York, N.Y. 1991, p.205-248
- [37] Sambrook J, Fritseh EF, Maniatis T. *Molecular cloning: a laboratory manual*. 2nd ed. Cold Spring Harbor Laboratory, New York, 1989, pp I.25–I.28.

- [38] Salvador-Pascual JJ, Collins-Martínez V, López-Ortíz A, Solorza-Feria O. Low Pt content on the Pd₄₅Pt₅Sn₅₀ cathode catalyst for PEM fuel cells. *Journal of Power Sources* 2010; 195, 3374-3379.
- [39] Suárez-Alcántara K, Solorza-Feria O. Evaluation of Ru_xW_ySe_z Catalyst as a Cathode Electrode in a Polymer Electrolyte Membrane Fuel Cell. *Fuel Cells* 2010; 10:84-92.
- [40] Velasquez-Orta SB, Curtis TP, Logan BE. Energy from algae using microbial fuel cells. *Biotechnology and Bioengineering* 2009; 103: 1068-1076.
- [41] Watson VJ, Logan BE. Analysis of polarization methods for elimination of power overshoot in microbial fuel cells *Electrochemical Communications* 2011; 13: 54-56.
- [42] Sathish-Kumar K, Solorza-Feria O, Hernández-Vera R, Vázquez-Huerta G, Poggi-Varaldo HM. Comparison of various techniques to characterize a single chamber microbial fuel cell loaded with sulfate reducing biocatalysts. *J. New Mat. Electrochem. Systems* 2012; 15: 195-201.
- [43] Aiba S, Ohishi M, Huang SY. *Ind. Eng. Chem. Fund* 1968; 7: 497–502.
- [44] Hwang ST, Tang TES, Kammermayer K. *J. Macromol Sci* 1971; 5: 1-10.
- [45] Refojo MF, Leong FL. Water-dissolved-oxygen permeability coefficients of hydrogel contact lenses and boundary layer effects. *Journal of Membrane Science* 1979; 4: 415-426.
- [46] Fatt I, Chaston J. Measurement of oxygen transmissibility and permeability of hydrogel lenses and materials. *International Contact Lens Clinic* 1982; 9: 76-88.
- [47] Brennan NA, Efron N, Holden BA. Oxygen permeability of hard gas permeable contact lens materials. *Clinical and Experimental Optometry* 1986; 69: 82-89.
- [48] Goldenberg MS, Rennwanz E, Beekman A, Polarographic Evaluation of Highly Oxygen Permeable Silicone Rubber: Correction for Electrode Nonlinearity and Implications for Contact Lenses. *International Contact Lens Clinic* 1991; 18:154-61.
- [49] Nasef MM, Zubir NA, Ismail AF, Dahlan KZM, Saidi H, Khayet M. Preparation of radiochemically pore-filled polymer electrolyte membranes for direct methanol fuel cells. *Journal of Power Sources* 2006; 156: 200-210.
- [50] Nasef MM, Zubir NA, Ismail AF, Khayet M, Saidi H, Dahlan KZM, Rohani R, Nagah TIS, Sulaiman NA. *Journal of Membrane Science* **2006**,;268: 96-108.

- [51] Kitada M, Lewis RJ, Krulwich TA. Respiratory chain of the alkalophilic bacterium *Bacillus firmus* RAB and its non-alkalophilic mutant derivative. *Journal of Bacteriology* 1983; 154: 330–335.
- [52] Tomlinson EJ, Ferguson SJ. Conversion of a c type cytochrome to a b type that spontaneously forms in vitro from apo protein and heme: Implications for c type cytochrome biogenesis and folding. *Proc. Natl. Academy of Science* 2000; 97: 5156–5160.
- [53] Sun D, Call D, Wang A, Cheng S, Logan BE. *Geobacter* sp. SD-1 with enhanced electrochemical activity in high-salt concentration solutions *Environmental Microbiology Reports* **2014**, DOI: 10.1111/1758-2229.12193.
- [54] Sorokin D.Y., T.P. Tourova, M. Mussmann, G. Muyzer, *Dethiobacter alkaliphilus* gen. nov. sp. nov., and *Desulfurivibrio alkaliphilus* gen. nov. sp. nov.: two novel representatives of reductive sulfur cycle from soda lakes *Extrem Life Extreme Cond* **2008**, 12: 431–439.
- [55] Pfeffer C, Larsen S, Song J, Dong M, Besenbacher F, Meyer RL, Kjeldsen KU, Schreiber L, Gorby YA, El-Naggar MY, Leung KM, Schramm A. Filamentous bacteria transport electrons over centimetre distances. *Nature* 2012; 491(7423): 218-221.
- [56] Carvalho ML, Doma J, Szttyler M, Beech I, Cristiani P. The study of marine corrosion of copper alloys in chlorinated condenser cooling circuits: The role of microbiological components. *Bioelectrochemistry* 2014; 97: 2-6.
- [57] Weber AK, Achenbach AL, Coates DJ. Microorganisms pumping iron: anaerobic microbial iron oxidation and reduction. *Nature Reviews Microbiology* 2006; 4:752-764.
- [58] Logan BE, Regan JM. Electricity-producing bacterial communities in microbial fuel cells. *Trends in Microbiology* 2006; 14: 512-518.
- [59] Holderoft S. Fuel Cell Catalyst Layers: A Polymer Science Perspective. *Chemistry of materials* 2014; 26: 381-393.
- [60] Nasef MM, Zubir NA, Ismail AF. Dahlan KZM, Saidi H, Khayet M. Preparation of radiochemically pore-filled polymer electrolyte membranes for direct methanol fuel cells. *Journal of Power Sources* 2006; 156(2): 200-210.

- [61] Molognoni D, Puig S, Balaguer M D, Liberale A, Capodaglio AG, Callegari A, Colprim J. Reducing start-up time and minimizing energy losses of Microbial Fuel Cells using Maximum Power Point Tracking strategy. *Journal of Power Sources* 2014; 269: 403-411.
- [62] Cheng S, Ye Y, Ding W, Pan B. Enhancing power generation of scale-up microbial fuel cells by optimizing the leading-out terminal of anode. *Journal of Power Sources* 2014; 248: 931-938.
- [63] Zuo Y, Cheng S, Logan BE. Ion Exchange Membrane Cathodes for Scalable Microbial Fuel Cells. *Environmental science & technology* 2008; 42: 6967-6972.
- [64] Orazem ME, Pébère N, Tribollet B. Enhanced Graphical Representation of Electrochemical Impedance Data. *Journal of the Electrochemical Society* 2006; 153: B129-B136.
- [65] Liang P, Huang X, Fan M.-Z, Cao XX, Wang C. Composition and distribution of internal resistance in three types of microbial fuel cells. *Appl Microbiol Biotechnol* 2007; 77: 551-558.
- [66] Miller L, Oremland R. Electricity generation by anaerobic bacteria and anoxic sediments from hypersaline soda lakes. *Extremophiles* 2008; 12(6): 837-848.
- [67] Paul VG, Minter SD, Treu BL, Mormile MR. Ability of a haloalkaliphilic bacterium isolated from Soap Lake, Washington to generate electricity at pH 11.0 and 7% salinity. *Environmental Technology* 2013; 35(8): 1003-1011.
- [68] Abrevaya X, Sacco N, Mauas PD, Cortón E. Archaea-based microbial fuel cell operating at high ionic strength conditions. *Extremophiles* 2011; 15 (6): 633-642.
- [69] Du Z, Li H, Gu T. A state of the art review on microbial fuel cells: A promising technology for wastewater treatment and bioenergy. *Biotechnology Advances* 2007; 25 (5): 464-482.
- [70] Mittal VO, Kunz HR, Fenton JM. Effect of Catalyst Properties on Membrane Degradation Rate and the Underlying Degradation Mechanism in PEMFCs. *Journal of the Electrochemical Society* 2006; 153: A1755-A1759.
- [71] Kusoglu A, Karlsson AM, Santare MH, Cleghorn S, Johnson WB. Mechanical response of fuel cell membranes subjected to a hygro-thermal cycle. *Journal of Power Sources* 2006; 161: 987-996.

- [72]Liu D, Case S. Durability study of proton exchange membrane fuel cells under dynamic testing conditions with cyclic current profile. *Journal of Power Sources* 2006; 162: 521–31.
- [73]Saito T, Merrill MD, Watson VJ, Logan BE, Hickner MA, Investigation of ionic polymer cathode binders for microbial fuel cells. *Electrochimica Acta* 2010; 55: 3398–3403.
- [74] Wei B, Tokash JC, Chen G, Hickner MA, Logan BE. Development and evaluation of carbon and binder loading in low-cost activated carbon cathodes for air-cathode microbial fuel cells. *RSC Advances* 2012; 2(33):12751-12758.
- [75] Fan Y, Sharbrough E, Liu H. Quantification of the Internal Resistance Distribution of Microbial Fuel Cells. *Environ. Science and Technology* 2008; 42: 8101-8107.
- [76]Choi TH, Won YB, Lee JW, Shin DW, Lee YM, Kim M, Park HB. Electrochemical performance of microbial fuel cells based on disulfonated poly(arylene ether sulfone) membranes. *Journal of Power Sources* 2012; 220: 269-279.
- [77]Pandit S, Ghosh S, Ghangrekar MM, Das D. Performance of an anion exchange membrane in association with cathodic parameters in a dual chamber microbial fuel cell. *Int. J. Hydrogen Energy* 2012; 37: 9383-9392.
- [78]Lim SS, Daud WRW, Jahim J, Ghasemi M, Chong PS, Ismail M. Sulfonated poly(ether ether ketone)/poly(ether sulfone) composite membranes as an alternative proton exchange membrane in microbial fuel cells. *Int. J. Hydrogen Energy* 2012; 37: 11409-11424.

Tables

Table 1. Thickness, water uptake, ionic exchange capacity and nanofiber deposition time for composite Nafion-PVA and SPEEK-PVA-PVB membranes, and for blend SPEEK-PVA membranes prepared in different solvents. Nafion[®] is included for comparison.

Membrane	Hydrated thickness (μm)	Water uptake (%)	IEC (meq/g)	Deposition time (h)
Nafion-PVA- 15	15 \pm 1	21.2 \pm 0.1	0.46	3
Nafion-PVA-23	23 \pm 2	21.8 \pm 0.1	0.35	6
SPEEK-35PVA(Water)	122 \pm 7	152 \pm 7	0.47	-
SPEEK-35PVA (DMAc)	185 \pm 3	490 \pm 12	0.71	-
SPEEK-PVA-PVB	102 \pm 12	93 \pm 9	0.31	15
Nafion-117 (commercial)	216 \pm 4	21.5 \pm 0.1	0.91	-

Table 2. Values of oxygen apparent transmissibility and permeability of the membranes measured experimentally by a potentiometric method at 25°C. The values represent the mean values after five measurements for each sample. The error is the standard deviation (SD).

Membrane	Thickness (μm)	I_{∞} (μA)	T_0 ^[a]	P ^[b] (Barrer)
Nafion-PVA-15	15 \pm 1	2.02 \pm 0.15	5.3 \pm 0.4	0.80 \pm 0.11
Nafion-PVA-23	23 \pm 2	1.66 \pm 0.12	4.4 \pm 0.3	1.01 \pm 0.16
SPEEK-35PVA (Water)	92 \pm 3	0.55 \pm 0.05	1.45 \pm 0.13	1.33 \pm 0.16
SPEEK-35PVA (DMAc)	89 \pm 3	0.33 \pm 0.03	0.87 \pm 0.08	0.77 \pm 0.10
SPEEK-30PVB- 35PVA	70 \pm 5	0.73 \pm 0.10	1.92 \pm 0.05	1.34 \pm 0.20
Nafion-117	183 \pm 5	2.4 \pm 0.3	6.3 \pm 0.8	11.5 \pm 1.8

[a] 10^{-8} cm³ of O₂ (STP) cm⁻² s⁻¹ cmHg⁻¹. [b] 1 Barrer: 10^{-10} (cm²/s)(cm³ of gas (STP)/cm³ of polymer/cmHg)

Table 3. Conductivity (σ) and characteristic number (β) calculated for each studied membrane. $\beta=\sigma/P$ is defined by the ratio of the proton conductivity of the membrane to its oxygen permeability.

Membrane	Thickness (μm)	σ (S/cm)	$\beta=\sigma/P$ (S's' cmHg cm ⁻³)
Nafion-PVA-15	15 \pm 1	(5.9 \pm 0.2) $\times 10^{-3}$	(7.4 \pm 1.3) $\times 10^7$
Nafion-PVA-23	23 \pm 2	(5.6 \pm 0.2) $\times 10^{-3}$	(5.5 \pm 1.1) $\times 10^7$
SPEEK-35PVA (Water)	92 \pm 3	(5.4 \pm 0.2) $\times 10^{-3}$	(4.1 \pm 0.6) $\times 10^7$
SPEEK-35PVA (DMAc)	89 \pm 3	(3.4 \pm 0.1) $\times 10^{-3}$	(4.4 \pm 0.2) $\times 10^7$
SPEEK-30PVB- 35PVA	70 \pm 5	(1.03 \pm 0.15) $\times 10^{-2}$	(7.69 \pm 2.3) $\times 10^7$
Nafion-117	183 \pm 5	(3.1 \pm 0.2) $\times 10^{-2}$	(2.7 \pm 0.2) $\times 10^7$

Table 4. Hybrid-H inocula molecular characterization results.

Similar clones	relative Identity (%)	Abundance (%)	Phylum (Class)
Archaea			
Methanococcus aeolicus (1)	100	25	Methanococci
Methanocaldococcus infernus(3)	99	75	Methanococci
Bacteria			
Geobacter metallireducens (1)	99	33	Delta bacterium
Marinobacter adhaerens (1)	100	33	Gammaproteo bacteria
Desulfurivibrio alkaliphilus (1)	100	33	Delta bacterium

Table 5. SCMFCs characterization with different Proton Exchange Membranes.

Type of Membrane	Current Density (mA/m ³) (mA/m ²)	Power Density (mW/m ³) (mW/m ²)	Voltage (mV)	Resistance = $R_{an}+R_{ca}+R_{mem+Sol}$ (Ω)
Nafion-117	3009 \pm 3 261 \pm 2	913 \pm 5 79 \pm 4	304 \pm 1	620+227+0.79
Nafion-PVA-15	3099 \pm 4 269 \pm 5	1053 \pm 2 91 \pm 1	340 \pm 1	427+94+0.53
Nafion-PVA-23	2465 \pm 9 214 \pm 3	642 \pm 7 55 \pm 7	260 \pm 1	2158+41+0.82
SPEEK-PVA-PVB	2817 \pm 8 245 \pm 1	813 \pm 1 70 \pm 3	288 \pm 1	1136+2+3.4
SPEEK-35PVA(Water)	2438 \pm 5 212 \pm 1	722 \pm 18 62 \pm 4	296 \pm 1	1460+1.9+4.4
SPEEK-35PVA(DMAc)	539 \pm 15 46 \pm 1	245 \pm 4 21 \pm 2	454 \pm 1	2311+20.63+8.17

Table 6. Comparison of the maximum power density deduced from polarization curves compared with previously values reported in literature.

Type of Membrane	Power Density (mW/m ³)	Cathode type	References
Nafion-117	913	Air Cathode	Our work
Nafion-PVA-15	1053	Air Cathode	Our work
Nafion-PVA-23	642	Air Cathode	Our work
SPEEK-PVA-PVB	813	Air Cathode	Our work
SPEEK-35PVA(Water)	722	Air Cathode	Our work
SPEEK-35PVA(DMAc)	245	Air Cathode	Our work
Disulfonated poly(arylene ether) sulfone)	616	Air Cathode	[76]
Nafion 212	488	Air Cathode	[76]
Anion Exchange Membrane	925	Air Cathode	[77]
Poly(ether sulfone)-SPEEK-5%	235	Air Cathode	[78]

List of Figures

Fig.1 Schematic illustration of the hybrid H-inocula procedure (after the third serial transfer of bio-electrolysis).

Fig. 2 SEM images of hybrid inoculum on the carbon cloth of anode where the presence of rod and cocci on the surface can be inferred.

Fig. 3 Cyclic voltammogram of hybrid inoculum on the anode carbon cloth electrode at different scan rates.

Fig. 4 Measured polarization and power density curves of the SCMFCs assembled with different PEMs.

Fig.5 EIS spectrum of the SCMFCs assembled with different PEMs. Insert the equivalent circuit used for the fitting of the experimental results.

Fig.6 Batch operation of microbial fuel cell loaded with Nafion-PVA 15 (a) and Nafion 117 (b).

Fig.7 EDAX characterization of NafionPVA15 (a) and Nafion 117 (b) after the batch operation of microbial fuel cell.

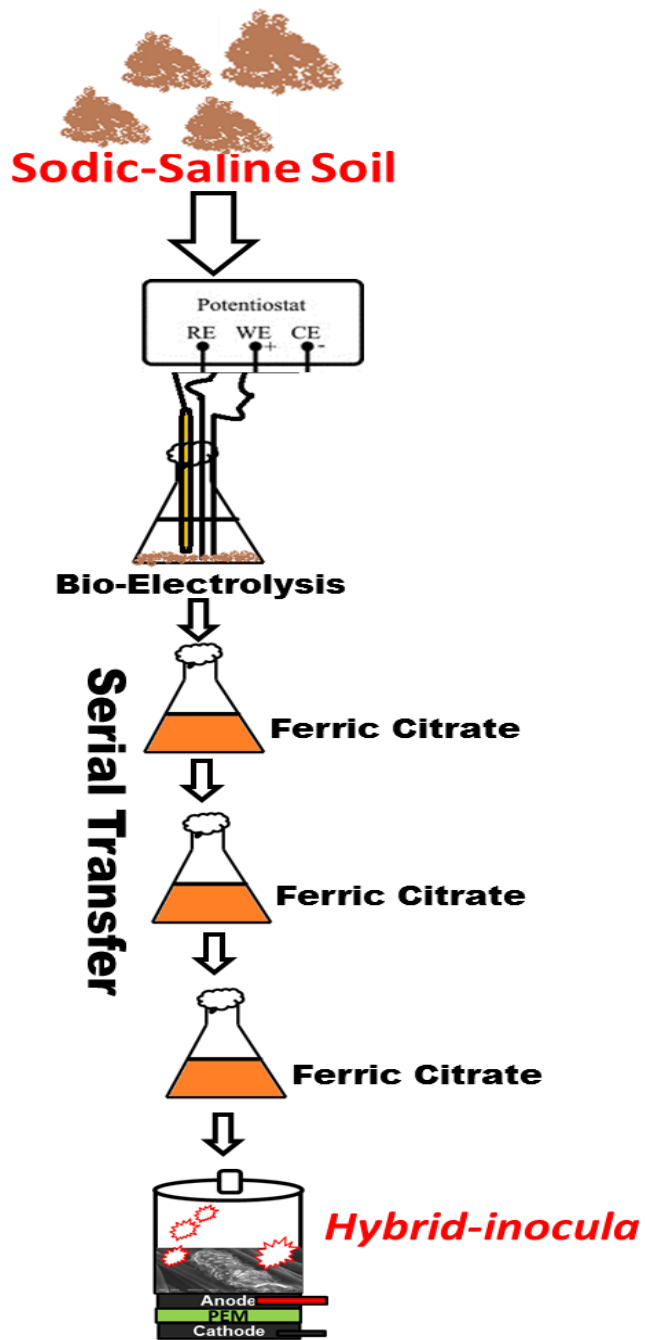


Figure 1

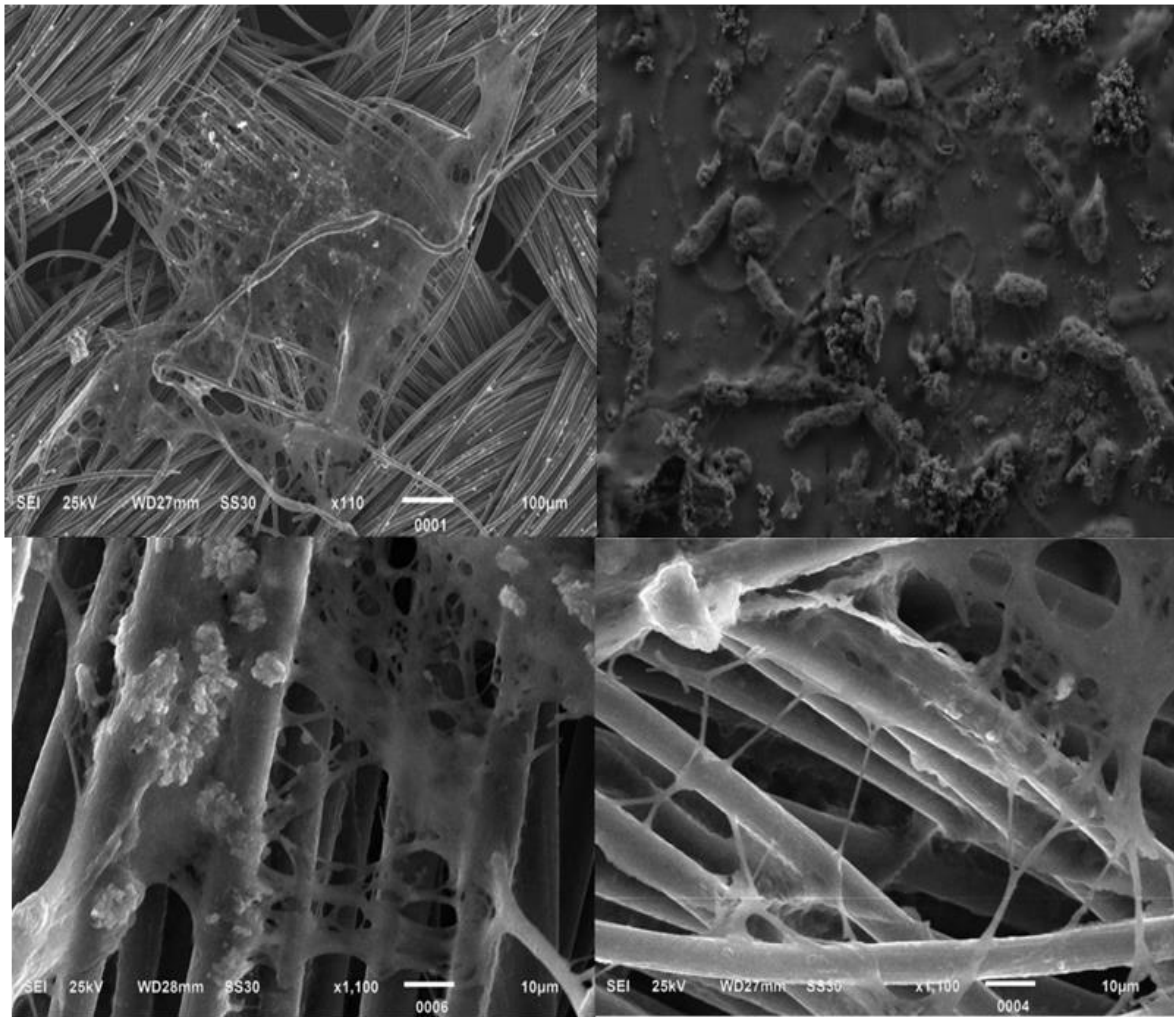


Figure 2

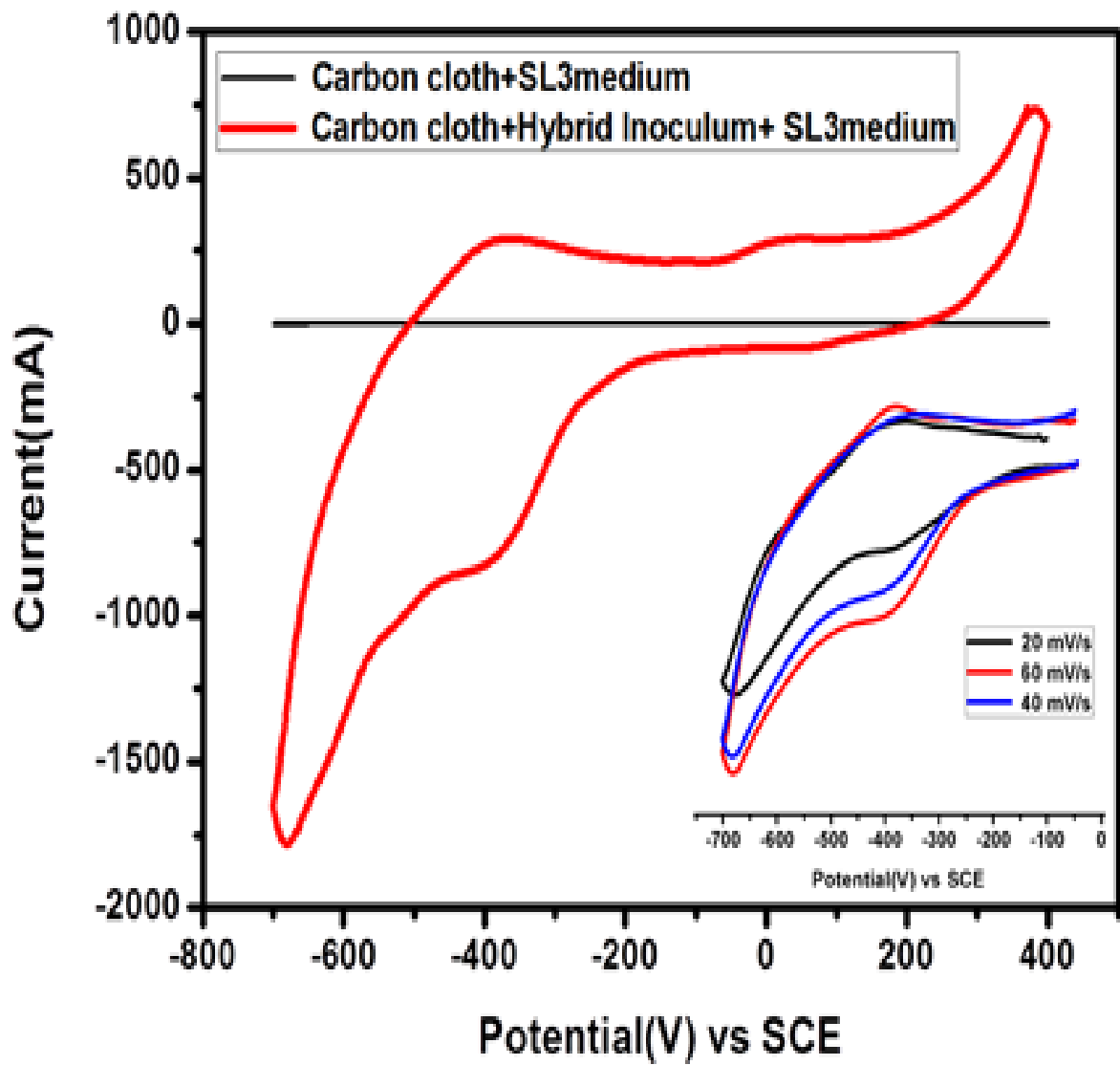


Figure 3.

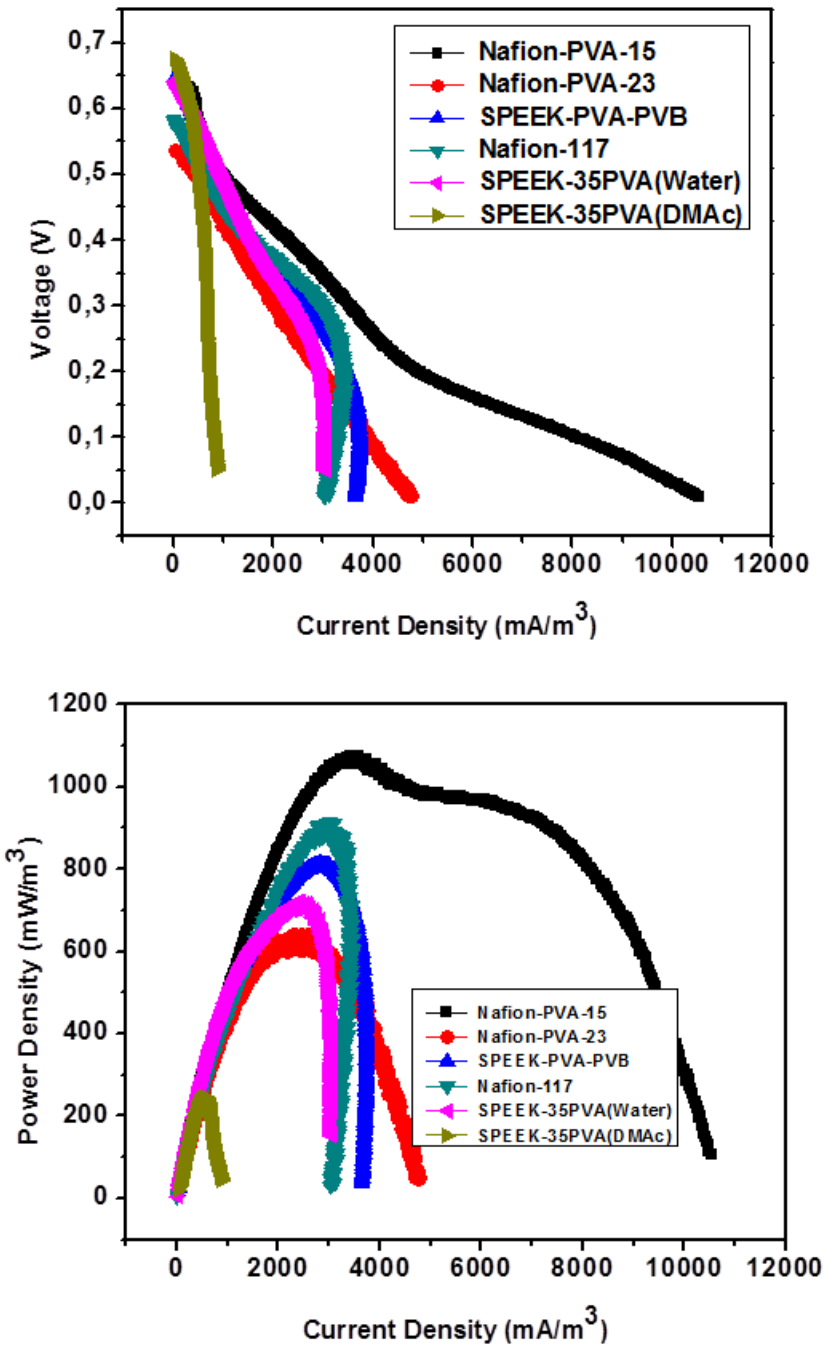


Figure 4.

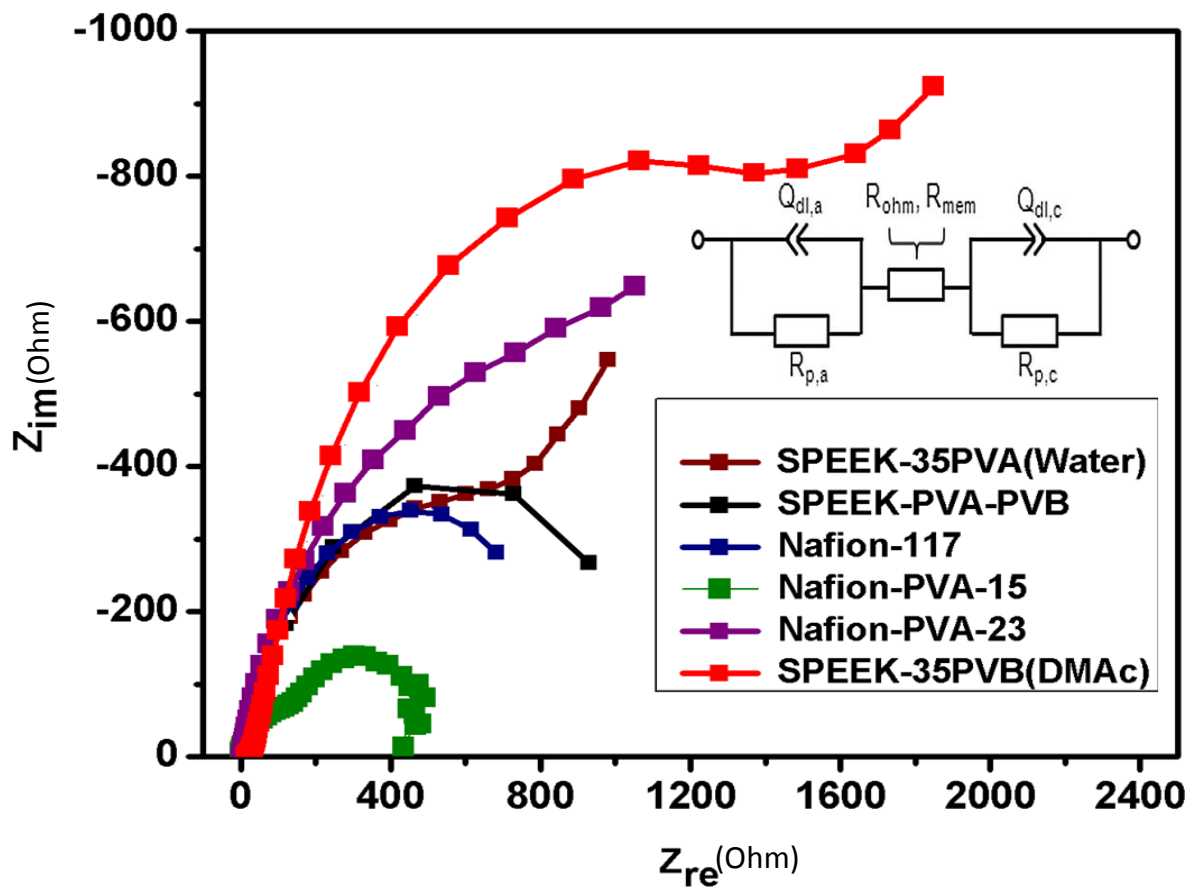


Figure 5.

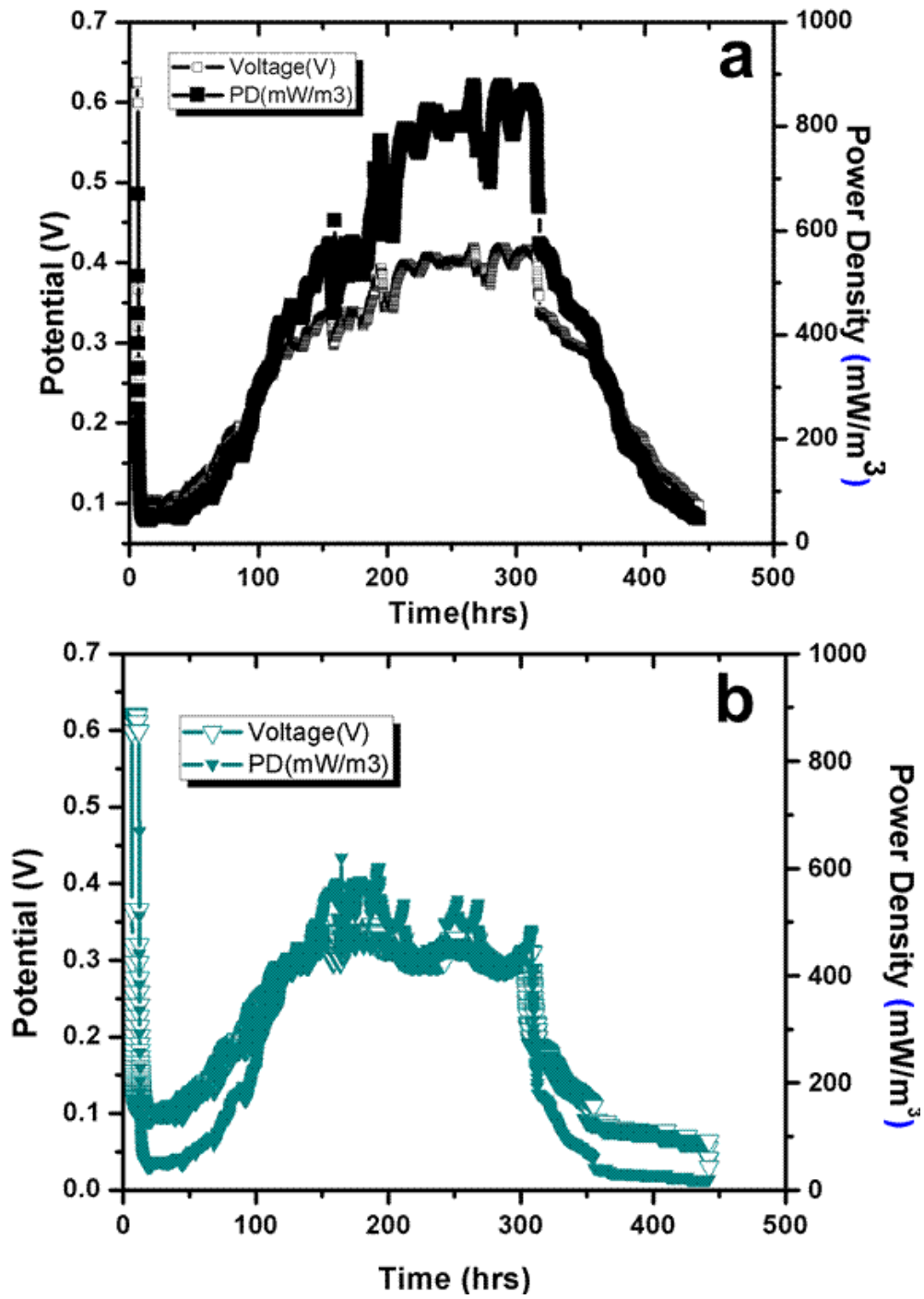


Figure 6.

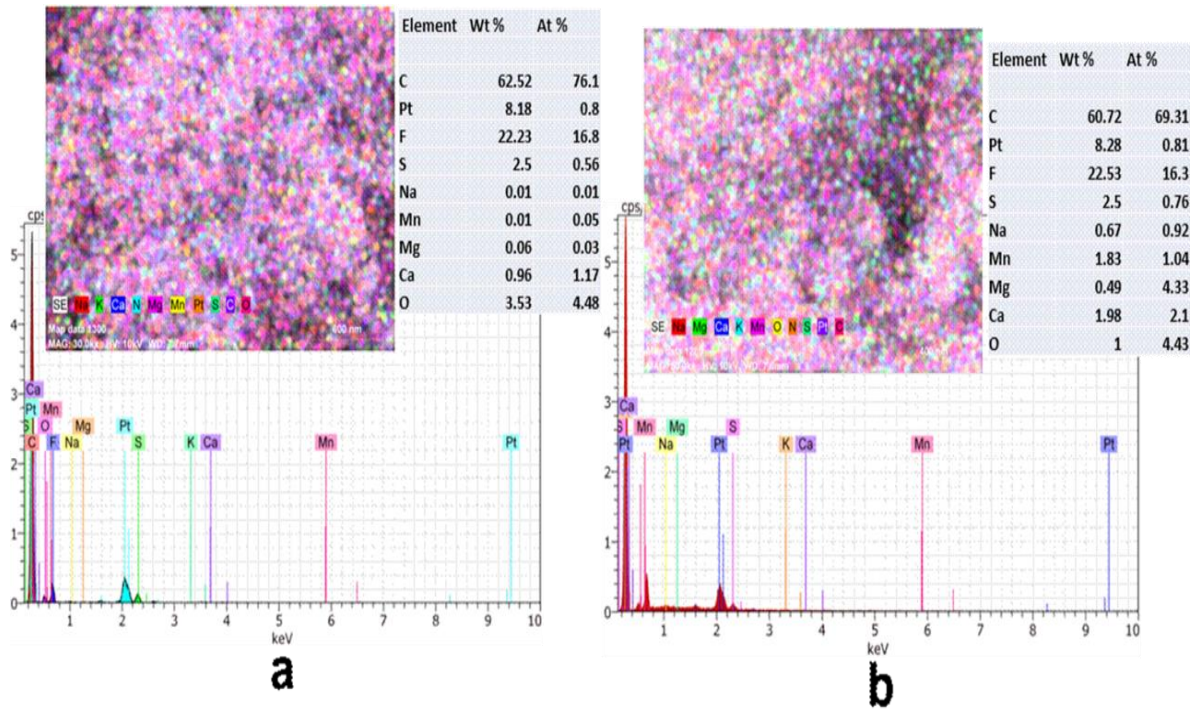


Figure 7.